Improved Target Method for AF-MPDT Thrust Measurement

IEPC-2015-172／ISTS-2015-b-172

Presented at Joint Conference of 30th International Symposium on Space Technology and Science
34th International Electric Propulsion Conference and 6th Nano-satellite Symposium,
Hyogo-Kobe, Japan
July 4 – 10, 2015

Baojun Wang[1], Haibin Tang[2], Wenjiang Yang[3], Mengdi Kong[4] and Yujie Xu[5]
Beihang University, Beijing, China

Abstract: This paper describes a target thrust measurement method for Applied-Field Magnetoplasmadynamic thruster (AF-MPDT). The thrust stand mainly consists of a target, an elastic beam, a displacement sensor, a movable platform and a damper. Its range and resolution can be adjusted by changing the thickness of the beam. A damper is designed to ensure that the target stabilizes rapidly. The movable platform is employed to ensure that the measurement position can be adjusted in the experiments. A direct calibration of the target has been performed with weights. Calibration curve of the thrust stand and thrust value of the thruster are given and analyzed. The thruster can provide a thrust of 183mN, under an input power of 6.3kW, an argon flow rate of 13.8mg/s, the applied field strength of around 0.2T.

I. Nomenclature

F = force acting on the target
s = displacement
E = Young's modulus
l = length of the beam
b = width of the beam
h = thickness of the beam
T = thrust
$\dot{m}$ = mass flow rate of propellant
v_e = exhaust velocity of the thruster plume
R = total static error of the thrust stand
R_n = repeatability error of the thrust stand
H_r = hysteresis error of the thrust stand
L_n = nonlinear error of the thrust stand

II. Introduction

AF-MPDT has the potential to be used as a primary propulsion system in high energy missions, such as deep-space exploring[1,2,3]. One of the most important performance parameter for AF-MPDT is thrust. But it is

[1]Ph.D student, School of Astronautics, wangbaojun@buaa.edu.cn.
[2] Professor, School of Astronautics, thb@buaa.edu.cn
[3] Associate professor, School of Astronautics, yangwjbuaa@sa.buaa.edu.cn
[4]Master, School of Astronautics, kongmengdi@buaa.edu.cn.
[5]Master, School of Astronautics, jetxu@buaa.edu.cn.

difficult to measure directly. In ground experiments, the mass of AF-MPDT is very large commonly while the thrust is relative small. It is a challenge for thrust stand to support so heavy thruster and to keep highly sensitive simultaneously. And the thruster will create massive thermal radiation and magnetic field when working, which will disturb measurement of thrust. Moreover, propellant feed lines and electric wires can generate unfixed disturbance force in the thrust direction, which is difficult to avoid [4, 5].

Because of so many difficulties in the direct thrust measurement, indirect thrust measurement may be a considerable choice. With the indirect method, only plume needs to be measured. The complexity of the thruster needs not to be considered anymore; measurement system becomes independent from thruster system.

Target thrust measurement, mounting a target in the direct path of the ejected propellant, is a typical indirect thrust measurement method. Some researchers have reported target methods, such as Ryoji Yanagi from the University of Tokyo, designed a cylindrical target for the measurement of impulse bits of Pulsed Plasma Thrusters [6]. Paolo Gessini from the University of Southampton designed a target thrust measurement system for ion thruster [4]. Hannah Bohrk from the University of Stuttgart performed TIHTUS thrust measurement with a baffle plate [7]. So far, however, there has been little discussion about target method for AF-MPDT, which has a different working mechanism from all of the above thrusters. Some researchers hold that part of acceleration process of AF-MPDT is finished outside of the thruster [8, 9]. It means that the velocity of the plume is not the largest, at export of the thruster. And the position where the plume gains the largest velocity changes with operation regime. To confirm the position, the thrust measurement position needs to be changeable, and that is very important for our experiments.

The target method can be classified into two types according to the ways installing the target. The target can be hanged or inverted. Hanging pendulums have the advantage of the simplicity of construction and high stability but need large enough space to install. Inverted pendulums have better sensitivity but worse stability. According to available experiment facilities, we choose the hanging scheme.

III. Experimental System

A. Vacuum System

The vacuum system consists of a vacuum tank, three class of pumping system, electrical control equipments and other peripheral equipments. The size of the vacuum tank is Φ1.8m×3.2m. The pumping system consists of four 2X-70A mechanical vacuum pumps, two ZJP-600 Roots pumps and two K-800 high vacuum oil diffusion pumps. The system, achieves an ultimate vacuum of 5.0×10-4 Pa and a working vacuum of 5.0×10-3 Pa when the propellant mass flow rate is lower than 30mg/s.

B. Thrust Stand

As shown in Fig.1 (left), the target method thrust measuring device consists of target, elastic beam, displacement sensors, movable platform and other components.

The elastic beam and target are fixed together, which are made of 304 stainless steel and mica respectively. The mica has favorable rigidity and adiabaticity that can reduce heat conduction from the target to the beam and thermal deformation of the target. The rigidity of the target is so large that it can be regarded as a rigid body; the rigidity of the beam is much smaller i.e. the beam can bend easily while the target deforms little, under the collision of the plume. It means obvious displacement of the target can be obtained, even though the thrust is relatively small.

Thruster plume impacts the target and bends the beam. The displacement of the beams can be measured by a laser displacement sensor, installed behind the beam. The resolution of laser displacement sensors can reach 0.5μm.

The beam has a rectangular section and the length is more than ten times to width. According to the theory of slender beams, force F and displacement s have following relationship [4].

$$s = -4l^3/(Ebh^3)*F \tag{1}$$

Where F is the force between the plume and the target, E, l, b and h are the Young's modulus, length, width and thickness of the beam respectively. E, b, l and h are constant keeping the temperature constant. A Linear relationship between F and s can be fund easily. The precondition of the slender beam theory is, the bend angle of the beam is less than 10° and the design angle is less than 5°.

The thrust of the AF-MPDT is decided by the following formula.

$$T=\dot{m}\upsilon_e \tag{2}$$

Where $\dot{m}$ is the mass flow rate of propellant, υ_e is the ejection velocity of thruster plume.

υ_e decreases to 0 m/s, after a collision between the plume and the target. Therefore, the following relationship can be obtained.

$$F=\dot{m}(\upsilon_e - 0) \tag{3}$$

Combining the above formulas, we get formula (4).

$$T = - Ebh^3 / (4l^3) * s \quad (4)$$

The displacement s can be measured with displacements sensor, and other parameters can be confirmed by calibrating the thrust stand. In this way the thrust value can be obtained.

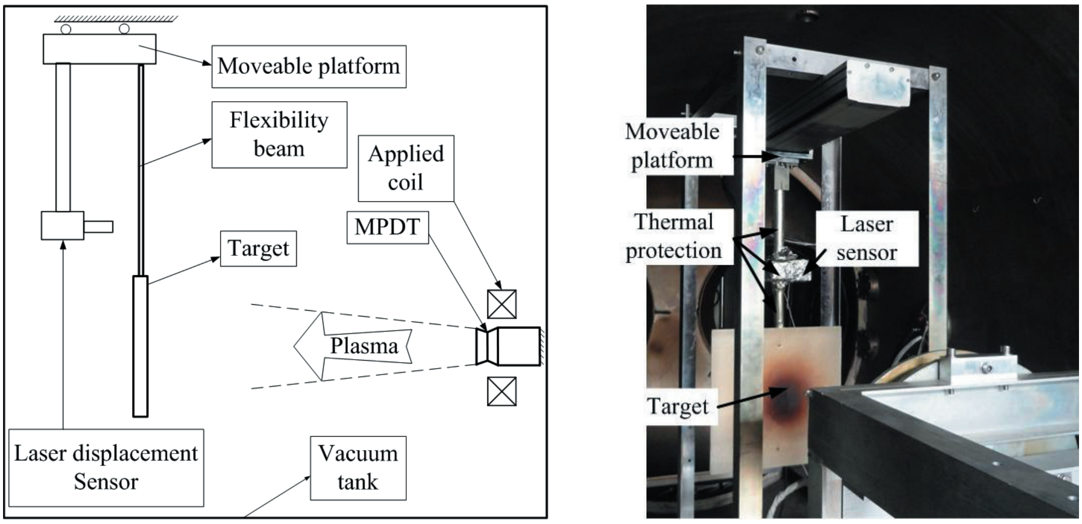

Figure 1 Schematic (left) and picture (right) of the trust stand

To make the thrust stand movable, the sensor, the beam, and the target are installed on a movable platform together. Thus, the position of the target can be adjusted conveniently in the process of the experiments. The position of the movable platform is controlled by guide screw, driven by servo motor. The precision of the platform is ±0.5mm, and the working stroke is 600mm. 600mm is long enough to find the largest velocity position if a suitable initial distance between the target and the thruster is chosen.

There are two measurement strategies according to the way moving the target. The first one is to move the target continuously without extinguishing the thruster and the second one is to close the thruster firstly and then move the target to the next position. Both schemes have been tried in the experiments. The advantage of the first scheme is to measure the thrust rapidly and the thrust values at every point in the working stroke can be obtained. However, the thermal influence is worse because the target needs to be dipped in the plume during the whole process. The advantage of the second scheme is the target can be cooled adequately. The thermal influence can be reduced to the lowest level. Nevertheless, thrust measure can be performed only in several selected position. Experiment data will be much fewer comparing with the first scheme. According to the experiment result, the second scheme gains better performance. Thus, it is employed as our final scheme.

C. Thermal Protection

When the AF-MPDT works, massive heat is created, much of which is absorbed by the target. And the heat will conduct the beam that can cause a change in Young's modulus E. It means that relationship between T and s is different from the calibration state. That can cause a significant error. To decrease the thermal influence, three strategies are employed. Firstly, the target is made of mica, a kind of insulation material. Mica can decrease the heat conduction from the target to the beam. Secondly, the beam is installed inside an alumina ceramics tube, covered with asbestos cloth. Both the ceramic and asbestos are insulation materials. As shown in Fig. 1(right), only a gap is left between the tube and the target; almost the entire beam is covered by the tube. Then the thermal radiation from the plume to the beam can be greatly reduced. Lastly, discontinuous experiments are employed. Duration for one measurement is limited to two minutes. The thrust stand can be cooled adequately between two measurements.

To ensure one thrust measurement can be finished within two minutes, a damper is employed. As shown in Fig. 2, damper consists of two pieces of aluminum plates and one bar magnet. The aluminum plates are fixed to the free end of the beam and oscillate together with the beam while the bar magnet is fixed to the vacuum tank. Once the beam is oscillating, there will be eddy current inside the plates that can attenuate the oscillation rapidly. As a result, the beam can stabilize rapidly. Moreover, the relative position of the plates and the magnet can be adjusted according to the need for the strength of the damping.

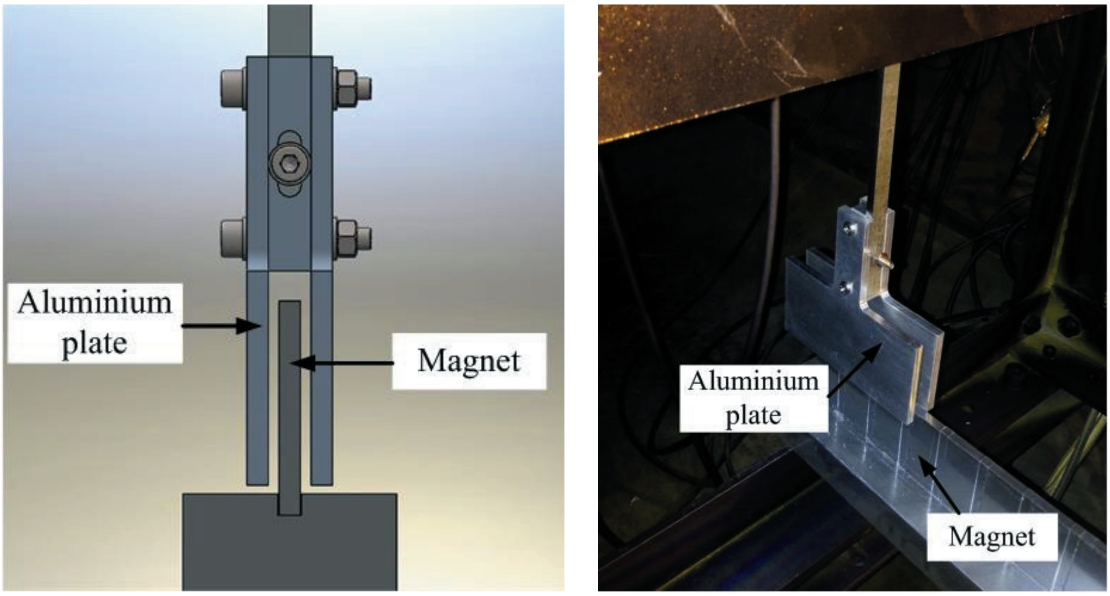

Figure 2 Schematic (left) and picture (right) of the damper

Besides the thermal protection for the beam, thermal protection for the displacement sensor is employed, too. The working temperature of the sensor, employed in the experiments, cannot be higher than 50℃. Therefore, thermal protection for the sensor is necessary. In the experiments, the sensor is installed inside a box, covered with plenty of asbestos cloth. The cloth can reduce the thermal radiation from the plume to the sensor greatly.

D. Calibration of the Thrust Stand

The purpose of calibration is to confirm the accurate relationship between displace *s* and standard force *F*. As shown in Fig. 3(left), standard force is loaded with weights. The output of thrust stand is voltage, corresponding to displacement *s*. The weights are connected to the center of the target with thin string. Different weights are loaded, and corresponding voltages are recorded. Calibration curves are shown in Fig.3 (right). According to that, we obtain the sensitivity which is 596mN/V.

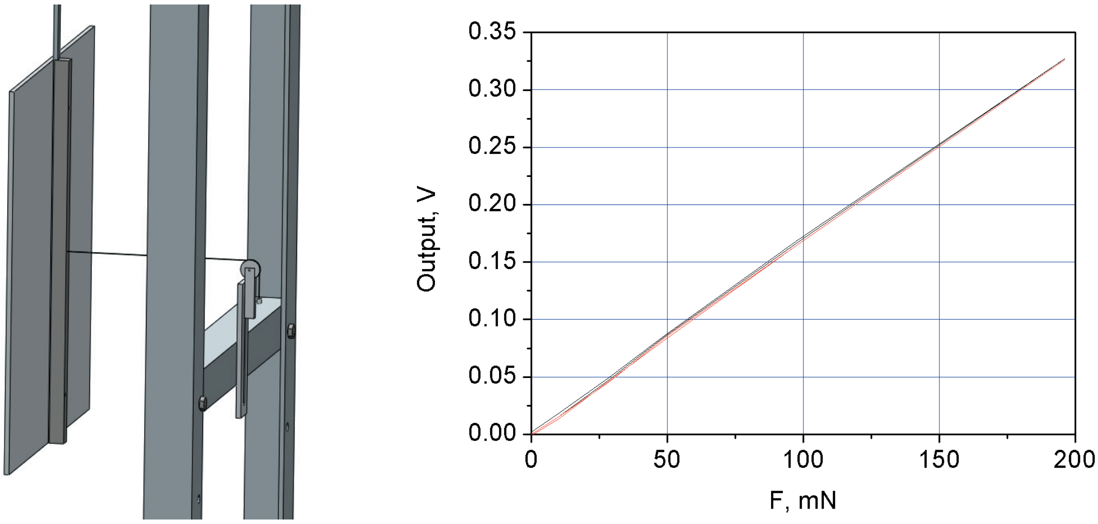

Figure 3 Schematic of calibration device (left) and calibration result (right)

IV. Result and Analysis

Fig.4 is the result of the experiments, measured with the thrust stand. The power of the thruster is 6.3kW; mass flow rate of propellant is 13.8mg/s with Argon; applied magnetic field strength is 0.2T; the largest thrust value is 183mN. The thrust is measured at seven different positions. The shortest distance between the target and the export of the thruster is 300mm and the longest distance is 750mm. The largest value is obtained at 400mm. As the distance increases, the measured values increase first and then decrease. It is easy to understand the trend of the curve between line B and line C, as shown in Fig. 4. When the target is far from the thruster, the target cannot prevent the entire plume since the plume has a divergence angle. However, the curve between line A and line B is an interesting phenomenon. It may mean the velocity of the plume reaches the highest value at 400mm, which can be explained by magnet nozzle theory. According to the theory, a part of the acceleration process is finished outside the thruster. And that need our further research.

The static error of the thrust stand can be evaluated by following formula.

$$R = \sqrt{R_n^2 + H_r^2 + L_n^2} \tag{5}$$

Where R_n is repeatability error; H_r is hysteresis error; Ln is nonlinear error.

According to the calibration results, R_n=0.9%; H_r =0.9%; L_n =1.4%; R=1.9%.

Besides the static error, there is an error caused by the thermal deformation. Though many strategies are employed for reducing the thermal influence, zero drift still exists, the value of which is 4.9%. Thus, the total error of the thrust stand is 5.2%.

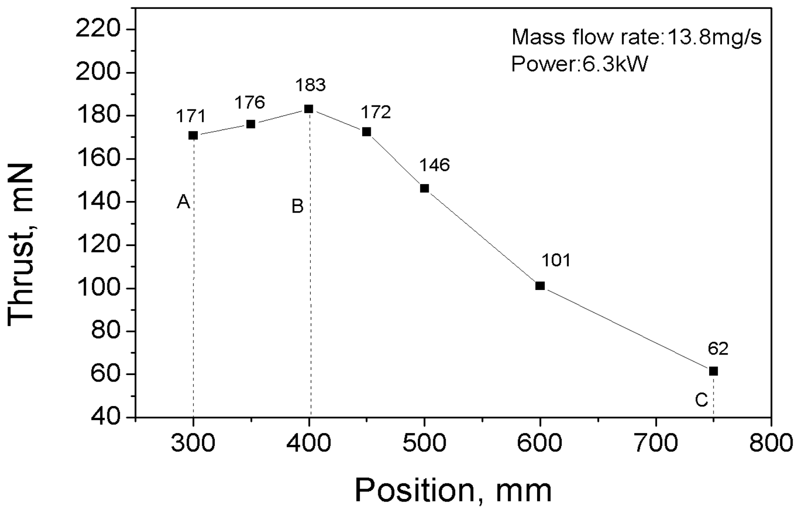

Figure 4 Thrust Value of AF-MPDT

V. Conclusion and Further Work

This article introduces a target thrust stand for AF-MPDT. The stand mainly consists of a flexible beam with a rectangular section, a rigid target made of mica and a laser displacement sensor. Both of them are installed on a movable platform to make sure that the measurement position can be adjusted during the experiments. To make the target stabilizes rapidly, a damper is designed. Three strategies are employed to reduce the thermal influence, caused by massive thermal radiation from the thruster. Firstly, adiabatic mica target is employed to reduce the heat conduction to the beam. Secondly, the beam is installed inside a ceramics tube to reduce the thermal radiation from the plume to the beam. Lastly, discontinuous experiments are employed to reduce the quantity of the heat absorbed by the target. The thrust is measured at seven different positions and the largest value of measured thrust is obtained at the distance of 400mm, from the thruster, rather than the nearest position. The thruster can provide a thrust of 183mN, under an input power of 6.3kW, an argon flow rate of 13.8mg/s, the applied field strength of around 0.2T. According to the experiment result, the movable thrust stand is proved to be an effective method for AF-MPDT thrust measurement. However, thermal influence is still significant, and further works are needed.

Acknowledgments

This work is supported by the National Natural Science Foundation of China (No.51276006).

References

[1]Kodys, A. and Choueiri, E. [2005] A Critical Review of the State-of-the-Art in the Performance of Applied-field Magnetoplasmadynamic

[2]Arakawa Y, Sasoh A, Arakawa Y, et al. Electromagnetic effects in an applied-field magnetoplasmadynamic thruster[J]. Journal of Propulsion & Power, 1992, 8(1):98-102.

[3]Mikellides P G, Turchi P J, Roderick N F. Applied-Field Magnetoplasmadynamic Thrusters, Part 1: Numerical Simulations Using the MACH2 Code[J]. Journal of Propulsion & Power, 2012, 16(5):887-893.

[4]Gessini P, Gabriel S B, Fearn D. Hollow cathode thrust measurement using a target: system calibration and development[J]. American Institute of Aeronautics & Astronautics, 2002.

[5]Grubisic A N, Gabriel S B. Development of an indirect counterbalanced pendulum optical-lever thrust balance for micro- to millinewton thrust measurement [J]. Measurement Science & Technology, 2010, 21(10):251-254.

[6]Yanagi R, Kimura I. New Type of Target for the Measurement of Impulse Bits of Pulsed Plasma Thrusters[J]. Journal of Spacecraft & Rockets, 2012, 19(3):246-249.

[7]Böhrk H, Auweter-Kurtz M. Thrust Measurement of the Hybrid Electric Thruster TIHTUS by a Baffle Plate[J]. Journal of Propulsion & Power, 2012, 25(3):729-736.

[8]INUTAKE M, ANDO A, HATTORI K, et al. Characteristics of a Supersonic Plasma Flow in a Magnetic Nozzle[J]. Journal of Plasmas&sfusion Research, 2002, 78(12):1352-1360.

[9]Lorzel H, Mikellides P G. Three-Dimensional Modeling of Magnetic Nozzle Processes[J]. Aiaa Journal, 2012, 48(7):1494-1503.